IMMUNOBIOLOGY

UV-inactivated HSV-1 potently activates NK cell killing of leukemic cells

Ismael Samudio,[1,2] Katayoun Rezvani,[3] Hila Shaim,[3] Elyse Hofs,[2] Mor Ngom,[2] Luke Bu,[4] Guoyu Liu,[4] Jason T. C. Lee,[2] Suzan Imren,[2] Vivian Lam,[2] Grace F. T. Poon,[2] Maryam Ghaedi,[2] Fumio Takei,[2] Keith Humphries,[2] William Jia,[4] and Gerald Krystal[2]

[1]Programa de Investigacion e Innovacion en Leucemia Aguda y Cronica, Bogotá, Colombia; [2]Terry Fox Laboratory, British Columbia Cancer Agency, Vancouver, Canada; [3]Department of Stem Cell Transplantation and Cellular Therapy, The University of Texas MD Anderson Cancer Center, Houston, TX; and [4]Brain Research Centre, University of British Columbia, Vancouver, Canada

Key Points

- UV-inactivated HSV-1 activates Toll-like receptor signaling in NK cells to kill leukemic, but not normal, allogeneic cells.
- UV-inactivated HSV-1 increases the therapeutic efficacy of allogeneic mononuclear cell infusions in a xenograft model of AML.

Herein we demonstrate that oncolytic herpes simplex virus-1 (HSV-1) potently activates human peripheral blood mononuclear cells (PBMCs) to lyse leukemic cell lines and primary acute myeloid leukemia samples, but not healthy allogeneic lymphocytes. Intriguingly, we found that UV light–inactivated HSV-1 (UV-HSV-1) is equally effective in promoting PBMC cytolysis of leukemic cells and is 1000- to 10 000-fold more potent at stimulating innate antileukemic responses than UV-inactivated cytomegalovirus, vesicular stomatitis virus, reovirus, or adenovirus. Mechanistically, UV-HSV-1 stimulates PBMC cytolysis of leukemic cells, partly via Toll-like receptor-2/protein kinase C/nuclear factor-κB signaling, and potently stimulates expression of CD69, degranulation, migration, and cytokine production in natural killer (NK) cells, suggesting that surface components of UV-HSV-1 directly activate NK cells. Importantly, UV-HSV-1 synergizes with interleukin-15 (IL-15) and IL-2 in inducing activation and cytolytic activity of NK cells. Additionally, UV-HSV-1 stimulates glycolysis and fatty acid oxidation–dependent oxygen consumption in NK cells, but only glycolysis is required for their enhanced antileukemic activity. Last, we demonstrate that T cell–depleted human PBMCs exposed to UV-HSV-1 provide a survival benefit in a murine xenograft model of human acute myeloid leukemia (AML). Taken together, our results support the preclinical development of UV-HSV-1 as an adjuvant, alone or in combination with IL-15, for allogeneic donor mononuclear cell infusions to treat AML. (*Blood*. 2016;127(21):2575-2586)

Introduction

Acute myeloid leukemia (AML) remains difficult to treat due to the reappearance of chemoresistant leukemic cells, even though most patients achieve a complete remission after first-line induction and consolidation chemotherapy. Although bone marrow transplantation (BMT) is considered to be a curative strategy for AML, 5-year disease-free survival after BMT remains <80% for the most favorable prognostic groups (inv16 or t[8;21]),[1] and only 35% of high-risk AML patients (complex karyotypes, monosomy, Flt-3 mutations, etc) survive 2 years after BMT.[2] More recent evidence suggests that survival may be improved by haploidentical natural killer (NK) cell transplants,[3,4] and strategies that augment the efficacy of NK-cell destruction of leukemic targets would thus be of utmost clinical importance.[5]

Herpes simplex virus-1 (HSV-1) is a large (>150 kb) double-stranded DNA oncolytic virus (OV) of the α-subfamily of *Herpesviridae* that has been engineered in various ways to preferentially infect and lyse transformed cells, leaving normal cells relatively unharmed.[6] Various OVs have shown excellent safety and promising therapeutic efficacy against solid tumors in a number of clinical trials,[7-14] and recently, Russell et al demonstrated that OV therapy may offer a therapeutic benefit for patients with hematologic malignancies.[15] The authors treated 2 measles-seronegative multiple myeloma (MM) patients with 1×10^{11} $TCID_{50}$ (50% tissue culture infectious dose) of an attenuated Edmonston measles vaccine strain engineered to express the sodium/iodide symporter (MV-NIS). Despite increased neutralizing viral antibody titers and decreased circulating viral mRNA in the weeks following MV-NIS administration, both patients exhibited a dramatic reduction in tumor burden, and 1 patient remained essentially free of MM for ≥6 months. It is thus intriguing to consider the possibility that durable responses in patients with hematologic malignancies may be possible with OV; however, in the absence of significant viral loads, and in the presence of high antibody titers, the mechanisms responsible for these responses remain to be elucidated.

NK cells are innate immune cells endowed with both antiviral and antitumor activity, in large part via the recognition of target cells that display "missing self" signals such as reduced HLA surface markers, or increased expression of "stress" signals such as major histocompatibility complex class I–related chain molecules A and B and UL16-binding proteins.[16] In addition to recognizing missing self or stress signals in tumors or virally infected cells, recent evidence suggests that NK cells can also recognize viruses themselves, as in the case of

Submitted April 13, 2015; accepted February 26, 2016. Prepublished online as *Blood* First Edition paper, March 3, 2016; DOI 10.1182/blood-2015-04-639088.

The online version of this article contains a data supplement.

There is an Inside *Blood* Commentary on this article in this issue.

The publication costs of this article were defrayed in part by page charge payment. Therefore, and solely to indicate this fact, this article is hereby marked "advertisement" in accordance with 18 USC section 1734.

cytomegalovirus (CMV; a β-subfamily member of *Herpesviridae*), which promotes the generation of memory-like NK cells in humans and mice that are transplantable, and have an increased interferon-γ (IFN-γ) and cytolytic response on encounter with target cells.[17,18] Notably, reactivation of CMV in BMT recipients has been associated with an antileukemic effect and a survival advantage,[19,20] supporting the notion that, because CMV is not oncolytic per se, viral reactivation or subclinical latent infections may promote antileukemic immunity. Interestingly, HSV-1 has been shown to directly stimulate CD69 and IFN-γ expression in NK cells via toll-like receptor 2 (TLR-2),[21] but there is no evidence to date that HSV-1 stimulates antileukemic immunity. Herein we report that UV light–inactivated oncolytic HSV-1 (UV-HSV-1), alone or synergistically with interleukin-15 (IL-15), potently stimulates the antileukemic activity of NK cells, in part via TLR-2/protein kinase C (PKC)/nuclear factor (NF)-κB signaling and metabolic reprogramming of carbon metabolism. Importantly, we provide evidence that this replication-defective vector may be used as an adjuvant ex vivo to increase the therapeutic efficacy of allogeneic donor mononuclear cell infusions.

Materials and methods

Cell lines, chemicals, and biochemicals

OCI-AML3 and Jurkat cells were maintained in RPMI-1640 medium supplemented with 10% fetal calf serum (FCS), 1% glutamine, 100 U/mL penicillin, and 100 μg/mL streptomycin in a 37°C incubator containing 5% CO_2. $CD34^+$ umbilical cord blood cells transduced with MN1 + ND13 oncogenes (MN1/ND13 cells)[22] were maintained in Iscove modified Dulbecco medium supplemented with 15% FCS, 1% glutamine, 100 U/mL penicillin, 100 μg/mL streptomycin, 10 ng/mL IL-3, 10 ng/mL granulocyte-macrophage colony-stimulating factor (GM-CSF), 10 ng/mL Flt-3, 10 ng/mL stem cell factor (SCF), and 10 ng/mL thrombopoietin. Foxp3 fixation and permeabilization buffers, CellTrace 450, CellTrace 670, anti-human CD56 conjugated to allophycocyanin (APC), anti-human CD34 conjugated to APC (clone 4H11), anti-human IFN-γ conjugated to e-Fluor 450, and anti-human CD69 conjugated to fluorescein isothiocyanate (FITC) were obtained from EBiosciences (San Diego, CA). Golgi Stop, Golgi Plug, and anti-human CD107a conjugated to FITC were obtained from BD Biosciences. IL-2, IL-3, GM-CSF, SCF, Flt-3 ligand, thrombopoietin, and IL-15 were from Peprotech (Rocky Hill, NJ). Pimonidazole and anti-pimonidazole adducts conjugated to FITC antibody were from Hypoxyprobe (Burlington, MA). Propidium iodide, 4',6-Diamidino-2-phenylindole dihydrochloride (DAPI), sodium cyanide, 2-deoxyglucose, and etomoxir were from Sigma-Aldrich (St. Louis, MO). Lactate scout strips and the portable lactate analyzer were from Sports Resource Group (Minneapolis, MN) and used to monitor lactate concentrations in culture supernatants as previously described.[23] Anti-human CD8 conjugated to phycoerythrin (PE), anti-human CD4 conjugated to FITC, Lymphoprep, phosphate-buffered saline (PBS), Hanks balanced salt solution (HBSS), CD32 (Fc receptor) blocking antibody, APC EasySep cell separation kits, FITC EasySep separation kits, and PE EasySep cell separation kits were from Stem Cell Technologies (Vancouver, Canada). PAM-3CSK (TLR-2 agonist), CLO-97 (TLR-7/8 agonist), double-stranded RNA (TLR-7 agonist), polyI:C (TLR-7 agonist), and cytosine guanine dinucleotide oligo (TLR-9 agonist) were from InvivoGen (San Diego, CA). All other chemicals were obtained of the highest purity available from Sigma-Aldrich.

Isolation of peripheral blood mononuclear cells and separation of CD4-, CD8-, or CD56-positive cells

Peripheral blood from healthy adult volunteers was collected under informed consent (REB protocol H12-00727) in EDTA vacutainer tubes and immediately diluted 1:1 with 23°C PBS. After mixing by inversion 15 to 20 times, 20 mL blood was overlaid on top of 10 mL Lymphoprep medium in 50-mL conical polypropylene tubes. Samples were then centrifuged at 800*g* for 20 minutes in a swing bucket Eppendorf 5804 centrifuge at 23°C. Centrifugation was allowed to stop without brake, and buffy coats were carefully collected and washed 3 times with PBS. Samples were finally resuspended in complete RPMI medium, and cell density was determined by hemocytometer counts of Trypan blue–negative cells. For isolation of CD56, CD8, or CD4 cells, peripheral blood mononuclear cells (PBMCs) were resuspended at a density of 1×10^8 cells/mL in PBS supplemented with 2% FCS and 1:10 dilution of CD32 blocking antibody, and incubated at 23°C for 5 min. Cell suspensions were then supplemented with 1.5 μg/mL of CD56-APC and further incubated at 23°C for 15 minutes, and target cells were isolated using EasySep kits per the manufacturer's instructions. CD56-depleted PBMCs were then used to EasySep isolate CD8-positive cells (using CD8-PE) or CD4-positive cells (using CD4-FITC). Purity of isolated cells was consistently >94% (98% for CD56-positive cells). Supplemental Table 1, available on the *Blood* Web site, lists the characteristics of the healthy donors used in this study.

Viral stocks and UV light inactivation

The HSV-1 vector was derived from HSV-1 strain 17+ by deletion of a repeat region and the ICP47 gene and placing the US11 open reading frame under the control of the ICP47 gene promoter. A CMV-driven green fluorescent protein (GFP) gene was cloned between the long unique and short unique regions, where the terminal repeat region occurs in the wild-type strain. This vector was named USGL-P25, and is referred to as HSV-1 throughout the paper. HSV-1 strain G207 was a kind gift of Neurovir (Vancouver, Canada). Vesicular stomatitis virus (VSV) expressing GFP was a kind gift from Paul Rennie (Prostate Cancer Centre, Vancouver General Hospital, Vancouver, Canada). Reovirus serotype 3 was a kind gift from Don Morris (University of Calgary, Calgary, Canada), and adenovirus-expressing enhanced GFP was a kind gift from Wilfred Jefferies (University of British Columbia, British Columbia, Canada). Viruses were UV inactivated by exposure to 20 J UV light (~10 minutes at maximal power output) using a Herolab UVT-M transluminator. Inactivation was confirmed by monitoring GFP/enhanced GFP expression and oncolytic potential against OCI-AML3 cells.

Virus treatment of PBMCs or purified CD56, CD8, or CD4 lymphocytes

PBMCs or purified CD56, CD8, or CD4 lymphocytes were resuspended in complete RPMI medium at a density of 3 to 4×10^6 PBMCs/mL. Cell suspensions were then treated with viruses at 0.0001 to 10 pfu/PBMC for varying periods of time, and floating and adherent cells were harvested (using cell-free dissociation buffer or PBS supplemented with 20 mM EDTA) and washed in complete RPMI medium twice.

Measurement of cytolytic activity by flow cytometry

Normal lymphocytes or OCI-AML3, Jurkat, or MN1/ND13 cells (1×10^6 cells) were washed once in HBSS (StemCell Technologies) and resuspended in 1 mL HBSS containing 10 μM of CellTrace 670. Cells were incubated at 37°C in a water bath for 15 minutes, followed by 3 washes in complete RPMI-1640 medium. Cells were then resuspended in 10 mL complete RPMI-1640 medium, and 50-μL aliquots per well were seeded in 96-well plates. Primary leukemia samples were thawed in the presence of DNase (50 μg/mL; Sigma-Aldrich), washed 3 times in HBSS supplemented with DNase (10 μg/mL), and resuspended in 1 mL HBSS containing 10 μM CellTrace 450. Primary leukemia cell suspensions were then incubated at 37°C in a water bath for 15 minutes, followed by washing and aliquoting as for the cell lines above. In some experiments, primary samples were seeded on top of the mesenchymal stromal cell (MSC) feeder layers (1000 MSCs per well). Sixteen hours after seeding of target cells (primary AML, normal lymphocytes, or cell lines), human PBMCs (or purified CD56 or CD8 lymphocytes) were added at the indicated ratios, and the cocultures were further incubated for 4 hours (24-48 hours for primary AML samples) in a 37°C incubator containing 5% CO_2. Cell line/PBMC/lymphocyte suspensions were collected into flow cytometry tubes containing 50 μL PBS supplemented with 4000 FITC- or PE-labeled Bioplex calibration beads (BioRad, Missisauga, ON, Cnada) and 10 μg/mL propidium iodide or DAPI. Primary samples/PBMC suspensions were washed once in PBS, incubated with CD32 blocking antibody (1:100 dilution in PBS; 50 μL) for 5 minutes at 23°C, and further incubated with anti-human CD34-APC–conjugated antibody

(1:100 dilution) for 15 minutes at 23°C. Cell line and primary sample cell suspensions were then washed once in PBS and analyzed by flow cytometry in a FACSCalibur cytometer (BD Biosciences) using 488- (beads and propidium iodide excitation) and 633-nm (Cell Trace 670) lasers, or a LSR Fortessa flow cytometer (BS Biosciences) using 405- (Cell Trace 450/DAPI), 488- (beads), 561- (beads/propidium iodide), and 640-nm (CD34/Cell trace 670) excitation lasers. Patient samples were analyzed by subgating on the $CD34^+$ cells from the Cell Trace 450 + gate. Results are expressed as % cell death; or % specific cell death using the following formula: % specific cell death = (% death in test sample − % death in control sample)/(100% − % death in control sample) × 100%; or (killed target cells – control dead cells)/1000 viable PBMCs.

Measurement of CD69 expression

After appropriate treatments, PBMCs were washed once with PBS, incubated with CD32 blocking antibody (1:100 dilution in PBS supplemented with 1 μg/mL propidium iodide; 50 μL) for 5 minutes at 23°C, and further incubated with anti-human CD56-APC (1:100 dilution) and anti-human CD69-FITC (1:100 dilution) conjugated antibodies for 15 minutes at 23°C. Cells were then washed once in PBS and analyzed by flow cytometry in a FACSCalibur cytometer using a 488-nm argon ion (CD69/propidium iodide) and 633-HeNe (CD56-APC) excitation lasers. Results are expressed as % positive cells for CD69 within the $CD56^+$ gate.

Measurement of intracellular IFN-γ and CD107a externalization

PBMCs (3×10^5 cells) were added to individual wells of a 96-well plate containing 10 000 Cell Trace 670–labeled OCI-AML3 cells. Cocultures were then supplemented with Golgi Stop (1:1000), Golgi Plug (1:1000), and anti-human CD107-FITC (5 μL/well) and incubated for 6 hours in a 37°C incubator containing 5% CO_2. Cell suspensions were collected, washed once in PBS, incubated with CD32 blocking antibody (1:100 dilution in PBS; 50 μL) for 5 minutes at 23°C, and further incubated with anti-human CD56-APC–conjugated antibody (1:100 dilution) for 15 minutes at 23°C. Cells were then washed once in PBS (supplemented with 2% FCS) and fixed and permeabilized using the Foxp3 fixation and permeabilization kit per the manufacturer's instructions. Fixed/permeabilized cells were stained for 1 hour at 23°C with 100 μL of a 1:100 dilution of anti-human IFN-γ conjugated to eFluor450 in permeabilization buffer. Stained cells were washed twice in PBS and analyzed by flow cytometry in an LSR Fortessa flow cytometer (BS Biosciences) using 405- (Cell Trace 450), 488- (CD107a), and 640-nm (CD56/Cell trace 670) excitation lasers. Target cells were at least a logarithm more fluorescent than CD56 bright cells, allowing adequate discrimination of target vs $CD56^+$ cells, which is essential because OCI-AML3 cells stain positive for both CD56 and CD107a (data not shown). Results are expressed as % CD107a-positive $CD56^+$ cells, % IFN-γ–positive $CD56^+$ cells, and mean fluorescent intensity of IFN-γ–positive $CD56^+$ cells.

Measurement of oxygen consumption by flow cytometry

Briefly, PBMCs were seeded in microfuge tubes (25-50 μL of a suspension of 1.0×10^7 cells/mL) in complete RPMI medium supplemented with pimonidazole (200 μM) and treated with 0.1 pfu/PBMC UV-HSV-1, 100 μM etomoxir, or both agents simultaneously. For the experiment presented in Figure 6F, EasySep purified CD56-positive cells were incubated in complete RPMI medium for 4 hours, and magnetic beads, which interfere with oxygen consumption measurements, were removed after several washes in complete medium. CD56-positive cells were then resuspended in complete RPMI medium (20 μL of a suspension of 1.0×10^7 cells/mL) and exposed to 0.1 pfu/cell UV-HSV-1, or not, as for PBMCs above. Cell suspensions were then immediately covered in light mineral oil and incubated for 4 hours at 37°C in a water bath. Sodium cyanide or sodium azide (6 mM)–treated samples served as controls to assess background and non-mitochondrial oxygen consumption. After incubation, a micropipette with tip was inserted through the mineral oil, taking care of expelling the oil that gets trapped, and the sample was recovered by slowly pipetting up and down several times, being careful not to collect any oil. Oil present on the outside of the pipette tip was wiped with a paper towel. Cells were collected by centrifugation (1200*g*, 5 minutes) and washed once in PBS. Cells were then incubated with CD32 blocking antibody (1:100 dilution in PBS; 50 μL) for 5 minutes at 23°C and further incubated with anti-human CD56-APC–conjugated antibody (1:100 dilution) for 15 minutes at 23°C. Cells were then washed once in PBS (supplemented with 2% FCS) and fixed and permeabilized using the Foxp3 fixation and permeabilization kit per the manufacturer's instructions. Fixed/permeabilized cells were stained for 1 hour at 23°C with 100 μL of a 1:400 dilution of anti-pimonidazole antibody (FITC conjugate) in permeabilization buffer. Stained cells were washed twice in PBS and analyzed by flow cytometry in a FACSCalibur cytometer using 488-nm argon ion (pimonidazole adducts) and 633-HeNe (CD56-APC) excitation lasers. Results are expressed as mean fluorescent intensity after subtracting the fluorescence intensity of the sodium cyanide (or sodium azide) control.

Migration assays

OCI-AML3–conditioned medium was prepared by resuspending 1 to 2×10^6 OCI-AML3 cells in 7 mL complete RPMI medium and incubating for 48 to 72 hours. Cells were then centrifuged, and conditioned media were filtered through a 0.2-μm filter. Conditioned media were stored at 4°C for ≤1 week; 500 μL conditioned media was placed at the bottom of 24-well plates, and 6.5-mm, 5.0-μm pore size Transwell permeable supports (Corning, Lowell, MA) were placed on top of the conditioned media, ensuring proper contact of the filter with the media. PBMCs ($2\text{-}4 \times 10^5$ cells) were added at 250 μL to the top of the filter, and plates were incubated for 2.5 h in a 37°C incubator containing 5% CO_2. Cell suspensions from the bottom of plate and top of permeable support were collected and added to separate flow cytometry tubes containing 100 μL PBS supplemented with 2% FCS and 4000 FITC- or PE-labeled Bioplex calibration beads. Cells were then centrifuged and resuspended in CD32 blocking antibody (1:100 dilution in PBS supplemented with 1 μg/mL propidium iodide; 50 μL) for 5 minutes at 23°C and further incubated with anti-human CD56-APC (1:100 dilution) antibody for 15 minutes at 23°C. Cells were then washed once in PBS, and absolute numbers of live $CD56^+$ lymphocytes were determined by flow cytometry in a FACSCalibur cytometer using 488-nm argon ion (beads/propidium iodide) and 633-HeNe (CD56-APC) excitation lasers. Results are expressed as % migration = [live $CD56^+$ cells at bottom of plate/(live $CD56^+$ cells at bottom of plate) + (live $CD56^+$ cells on top of permeable support)] × 100%.

Measurement of triglyceride content

After appropriate treatments, PBMCs were loaded with LipidTox neutral green stain (1:200; Invitrogen, Carlsbad, CA) for 45 minutes in a 37°C incubator, followed by staining with anti-human CD56-APC for 15 minutes at 23°C. After 2 washes in PBS, fluorescent emission at 525 nm was analyzed by flow cytometry in a FACSCalibur cytometer using 488-nm argon ion (LipidTox) and 633-HeNe (CD56-APC) excitation lasers. Results are expressed as mean fluorescent intensity.

Primary samples

Frozen bone marrow or peripheral blood samples from patients with AML and frozen bone marrow–derived MSCs from normal donors were obtained from the hematology cell bank at the BC Cancer Agency under REB protocol H12-00727. Supplemental Table 2 summarizes the clinical characteristics of the AML samples used. All experiments with primary AML samples were performed in triplicate, and only AML samples exhibiting baseline viability >50% were used in this study.

Mice

NOD-Rag1^{null} IL-2Rγc^{null} male mice producing human IL-3, GM-CSF, and SCF (NRG-3GS mice derived from NSG-3GS mice[24]) were bred in the animal resource center at the British Columbia Cancer Research Centre. All mouse experimental procedures were carried out in accordance with Canadian Council on Animal Care guidelines with approval from the University of British Columbia.

Leukemia model

Fifteen NRG-3GS mice (average age, 15 weeks) were sublethally irradiated with 315 cGy of ^{137}Cs γ-rays at 3.75 cGy/minute at 16 hours prior to being injected intravenously (i.v.) with 5×10^5 MN1/ND13 cells as previously described.[22] Twenty-eight days after implantation, engraftment was verified by flow cytometry, and animals were assigned to 3 groups as follows: group 1, PBS, 5 mice, each received 200-μL injections of PBS i.v.; group 2, PBMCs, 5 mice, each received 3×10^6 human T cell–depleted PBMCs (in 200 μL of PBS i.v.);

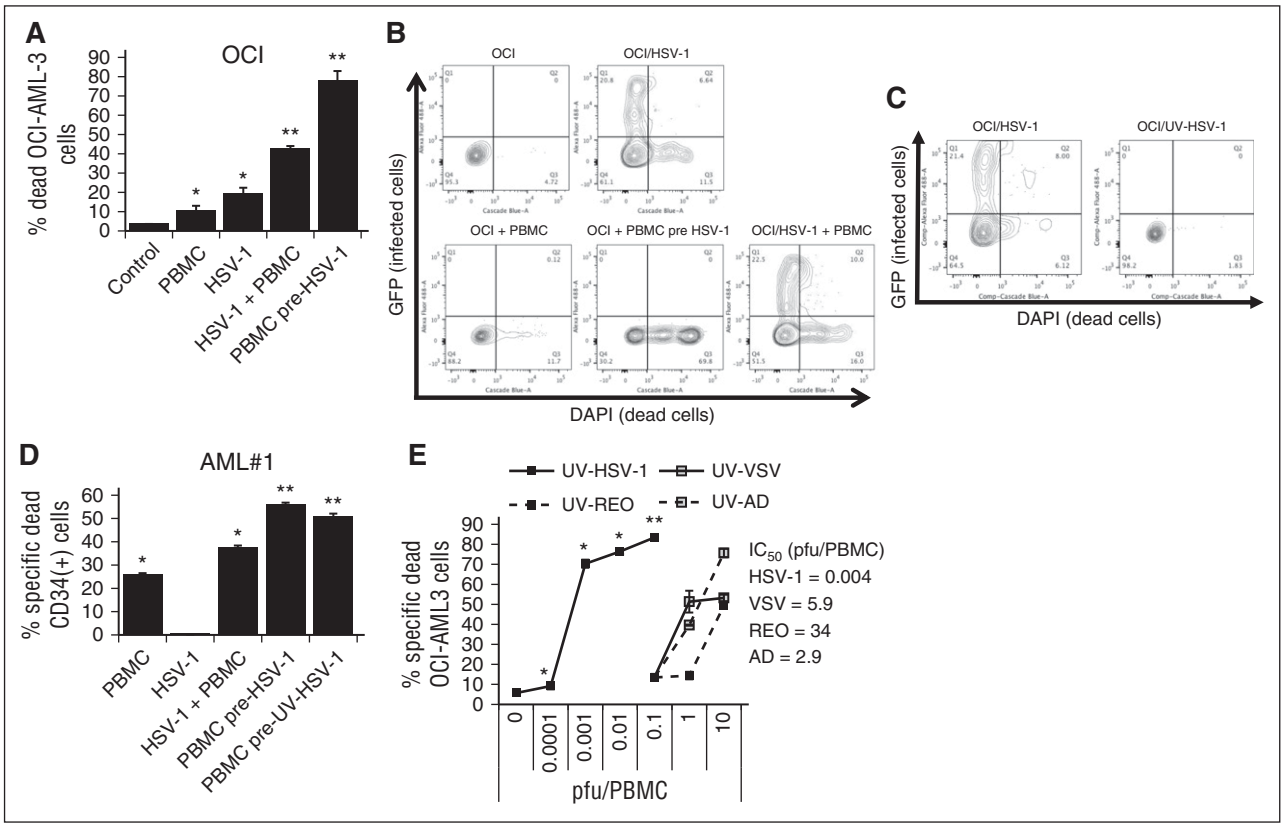

Figure 1. HSV-1 potently stimulates PBMC to kill leukemic cells. (A) Percent dead OCI-AML3 cells determined by flow cytometry as described in "Materials and methods" after culture with PBMCs or PBMCs pre-exposed for 16 hours to 0.1 pfu/PBMC HSV-1 (30:1 effector:target). *$P < .05$ from control; **$P < .0001$ from PBMCs alone. (B) Representative flow cytometry plots of OCI-AML3 cells infected or not with HSV-1, ±PBMCs or PBMCs pre-exposed to HSV-1. (C) Representative flow cytometry plots of OCI-AML3 cells exposed to live or UV-inactivated HSV-1. (D) Percent dead $CD34^+$ primary leukemic cells determined by flow cytometry as described in "Materials and methods" after culture with PBMCs or PBMCs pre-exposed for 16 hours to 0.1 pfu/PBMC of HSV-1 or UV-HSV-1 (30:1 effector:target). *$P < .01$ from control; **$P < .001$ from PBMCs alone. (E) PBMCs were exposed to increasing concentrations of UV-inactivated viruses for 16 hours. Cytolytic activity against OCI-AML3 cells was determined as in B. *$P < .05$ from PBMCs alone; **$P < .05$ from VSV, Reo, or Ad at 10 pfu/PBMC.

group 3, PBMCs + UV-HSV-1, 5 mice, each received 3×10^6 human PBMCs that had been exposed to 0.1 pfu/PBMC of UV-HSV-1 for 16 hours (washed 2 times in complete media, once in PBS, and resuspended in 200 μL of PBS for i.v. injection). T-cell depletion was performed using the RosetteSep human CD3 depletion cocktail per the manufacturer's instructions (StemCell Technologies). Leukemia engraftment was monitored by flow cytometry by quantitating GFP/yellow fluorescent protein (YFP) abundance within the live lymphocyte/monocyte population. Survival was estimated by Kaplan-Meier curves and analyzed for statistical significance using the log-rank (Mantel Cox) test in GraphPad Prism software (La Jolla, CA).

Statistics

Unless otherwise indicated, results are expressed as mean ± standard deviation of ≥3 independent experiments. All experiments using cell lines or MN1/ND13 umbilical cord blood–transformed cells were performed in triplicate and repeated at least twice. *P* values were determined by unpaired Student *t* test or by a pairwise *t* test when comparing differences across various healthy donors. $P < .05$ was considered significant.

Results

HSV-1 potently stimulates PBMCs to kill leukemic cells

To explore whether HSV-1 could stimulate innate immunity against leukemia cells, we exposed the human AML cell line OCI-AML3, or not, to GFP-expressing HSV-1 (1 pfu/cell), alone or in the presence of PBMCs for 48 hours. As well, to determine whether HSV-1 was directly killing OCI-AML3 cells or stimulating PBMCs to induce cytolysis of leukemic cells, OCI-AML3 cells were also cultured for 48 hours with PBMCs that had been previously exposed to, and washed free of, GFP-expressing HSV-1 (0.1 pfu/PBMC; 16-hour pre-exposure). Intriguingly, as shown in Figure 1A, PBMCs previously exposed to HSV-1 were more effective than PBMCs alone or PBMCs continuously exposed to HSV-1 in inducing cytolysis of OCI-AML3 cells. Moreover, as shown in Figure 1B, flow cytometric analyses demonstrated expression of GFP in OCI-AML3 cells exposed to HSV-1, indicating that these cells are permissive to infection, but GFP expression was not detected in OCI-AML3 cells cultured with PBMCs previously exposed to HSV-1, suggesting that in the absence of permissive infection, PBMCs are stimulated by HSV-1 to become very robust killers of leukemia cells. Consistent with this notion that infectivity is not required to stimulate a robust innate antileukemic immune response, similar results were observed using UV-HSV-1, as shown in Figure 1C-E.

Herpesviridae family members may be unique in promoting immune responses against leukemic cells, based on data showing an antileukemic benefit of CMV reactivation in posttransplant patients.[19,20] To address this possibility, we compared the cytolytic response of PBMCs incubated with varying doses of UV-HSV-1, to UV-inactivated VSV (UV-VSV), Reovirus (UV-REO), and Adenovirus (UV-AD). Strikingly, UV-HSV-1 was ~1000-fold more potent than UV-AD and UV-VSV and ~10 000-fold more potent than UV-REO in stimulating

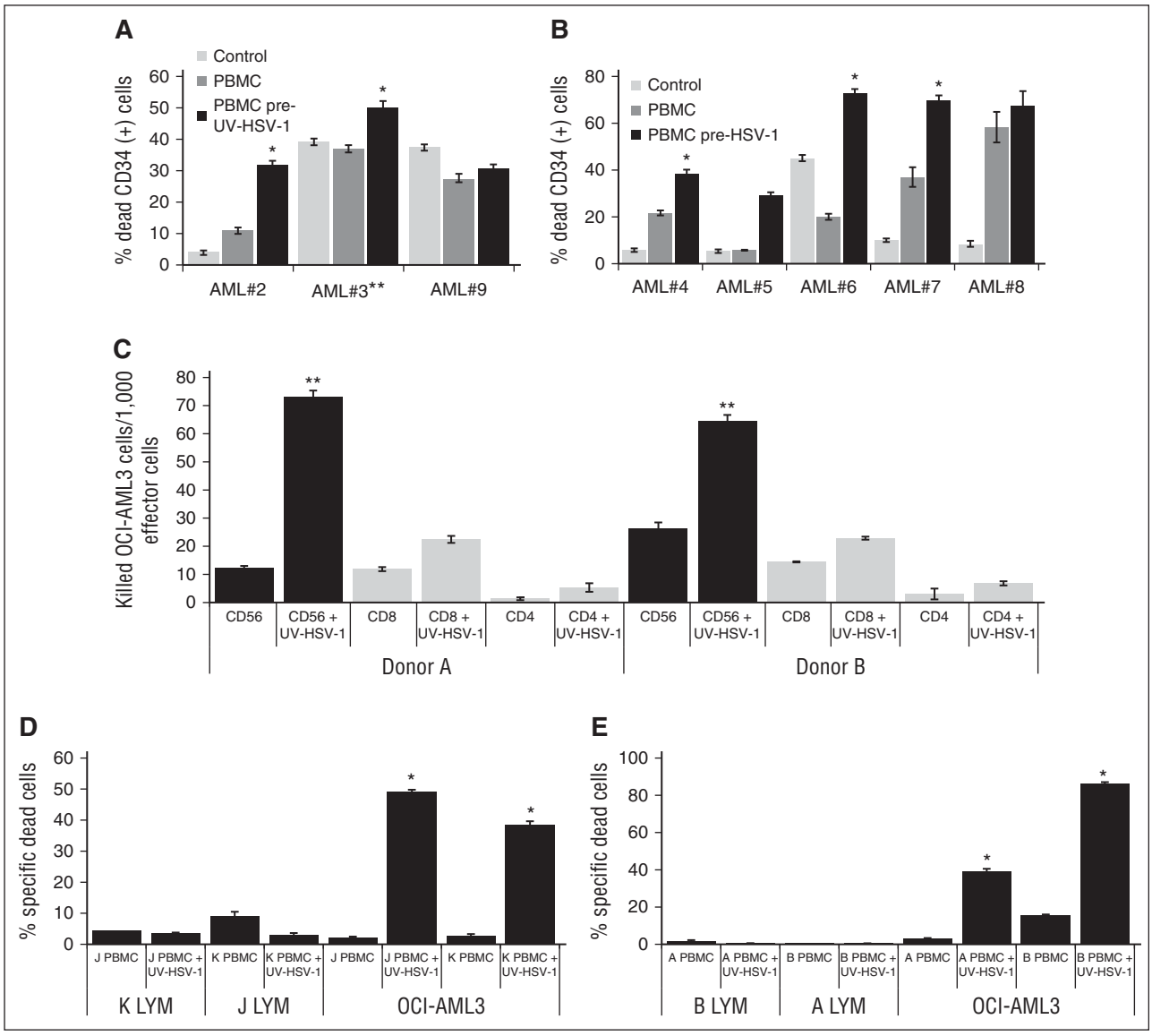

Figure 2. HSV-1 or UV-HSV-1 stimulates NK-dependent cytolysis of primary AML cells or cell lines but not of allogeneic healthy lymphocytes. (A) PBMCs exposed, or not, to UV-HSV-1 (0.1 pfu/PBMC for 16 hours) were added to primary AML cells (30:1 effector:target) cultured on MSC feeder layers (except 3, which was cultured alone). Cocultures were incubated for 48 hours, and % dead $CD34^+$ cells were determined by flow cytometry as described in "Materials and methods." (B) PBMCs exposed, or not, to live HSV-1 were added to primary AML cells, and % dead $CD34^+$ cells were determined after 48 hours as above. *$P < .005$ from PBMCs alone. (C) CD56-, CD4-, and CD8-positive cells were purified from 2 healthy donors by EasySep methodology as described in "Materials and methods." Isolated cells were then exposed, or not, to UV-HSV-1 (0.1 pfu/PBMC) for 16 hours and tested for their cytolytic activity against OCI-AML3 cells, and the results are expressed as killed OCI-AML3 cells per 1000 effector lymphocytes. **$P < .001$ from CD4 or CD8, UV-HSV-1–exposed lymphocytes. (D-E) Healthy PBMCs were exposed, or not, to UV-HSV-1 as above, and their cytolytic activity (30:1 effector to target ratio) against OCI-AML3 or healthy allogeneic lymphocytes (from the other donor tested in each graph) was determined as described in "Materials and methods." *$P < .0001$ from unexposed PBMCs.

PBMCs to kill OCI-AML3 cells (Figure 1E), and similar results were observed with PBMCs from several healthy PBMC donors (data not shown). In addition, we compared our strain of HSV-1 (USGL-P25 derived from strain 1716) to G207, another strain of HSV-1 derived from strain F, and observed that both viruses significantly ($P < .01$) enhanced PBMC-induced cytolysis of Jurkat and OCI-AML3 cells at 0.1 pfu/PBMC (supplemental Figure 1A). Last, during the revision of this manuscript, it was observed that exposure of PBMCs to UV-inactivated CMV did not increase their cytolytic potential (supplemental Figure 1B) and did not promote CD69 upregulation on the surface of $CD56^+$ cells (supplemental Figure 1C), suggesting that the beneficial effects of CMV reactivation in leukemia BMT recipients are likely mediated by adaptive NK cells, rather than NK cell activation per se. These data suggest that members of the α-subfamily of *Herpesviridae* uniquely enhance innate immunity against a variety of hematologic malignancies.

HSV-1 stimulates PBMC cytolysis of primary AML cells cultured alone or with MSCs

MSCs promote survival of AML cell lines and primary samples.[23] We therefore asked whether the cytolytic efficacy of PBMCs previously exposed to HSV-1 or UV-HSV-1 against AML primary samples would be compromised by MSC feeder layers. Exposure of PBMCs for 16 hours to 0.1 pfu/PBMC of UV-HSV-1 (Figure 2A) or HSV-1 (Figure 2B) promoted a significant ($P < .01$) increase in cytolysis in 5 of 7 AML samples cultured on MSC feeder layers (AML 3 was cultured alone). As observed for allogeneic healthy lymphocytes,

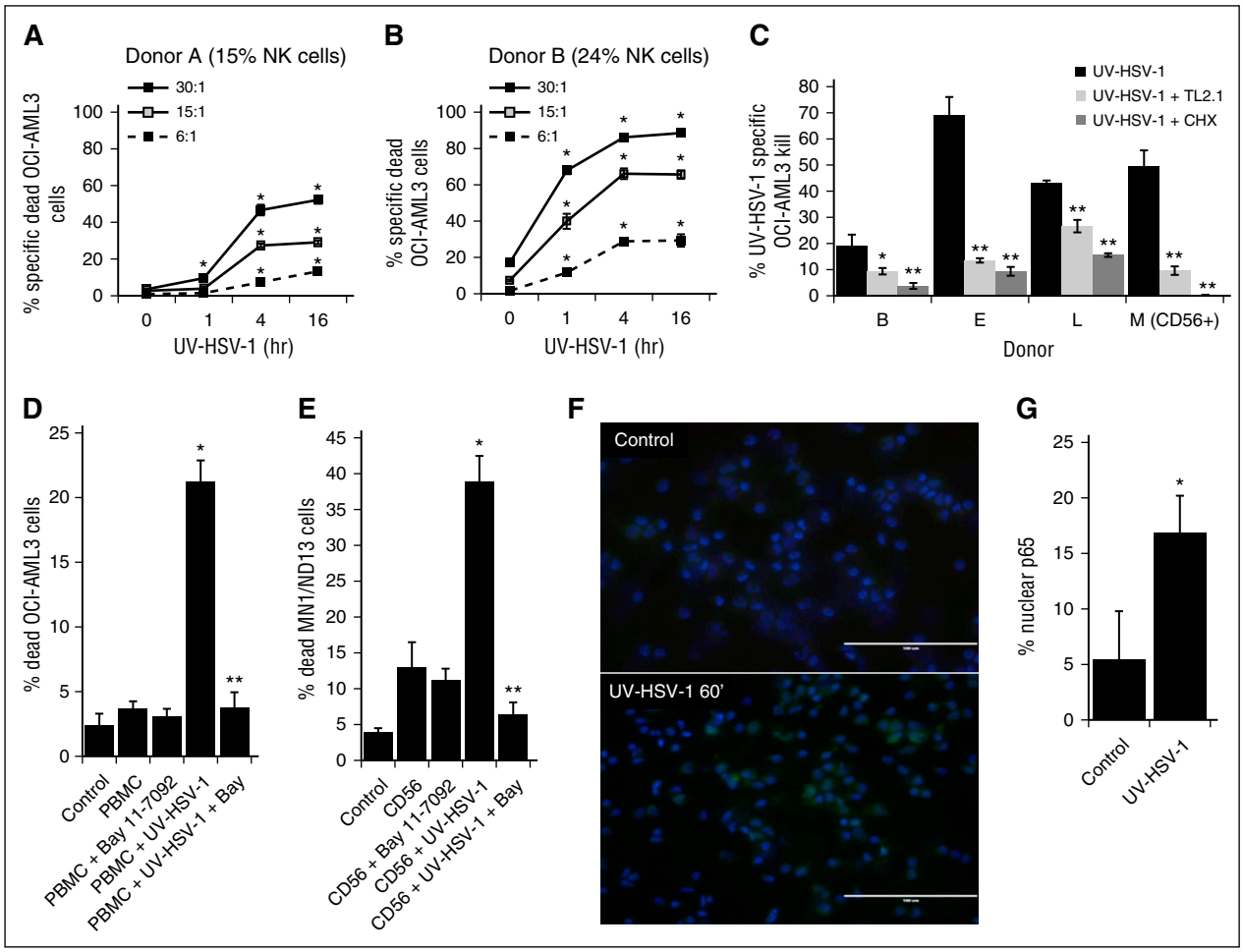

Figure 3. UV-HSV-1 rapidly stimulates the cytolytic activity of PBMCs in a TLR-2/NK-κB–dependent manner. (A-B) PBMCs from 2 healthy donors were exposed to UV-HSV-1 (0.1 pfu/PBMC) for 1, 4, and 16 hours, and their cytolytic activity against OCI-AML3 cells at the indicated effector:target ratios was determined. $^*P < .01$ from time 0. (C) PBMCs from 3 healthy donors, or purified NK cells from 1 donor (donor M), were exposed to UV-HSV-1 (0.1 pfu/cell for 16 hours), ±anti–TLR-2 antibody (clone TL2.1; 10 μg/mL for donors B and L, 15 μg/mL for donors F and M), or cycloheximide (CHX; 10 μg/mL), and their cytolytic activity (30:1 effector:target) against OCI-AML3 cells was determined. $^*P < .05$ from UV-HSV-1 alone; $^{**}P < .01$ from UV-HSV-1 alone. (D) Healthy PBMCs were exposed to UV-HSV-1 (0.1 pfu/PBMC for 16 hours), ±1 μM Bay-11-7082, and their cytolytic activity (30:1 effector:target) against OCI-AML3 cells was determined. $^*P < .01$ from unexposed PBMCs; $^{**}P < .01$ from PBMC + UV-HSV-1. (E) Purified NK cells were exposed or not to UV-HSV-1 (0.1 pfu/PBMC for 16 hours), ±1 μM Bay-11-7082, and their cytolytic activity (10:1 effector:target) against OCI-AML3 cells was determined. $^*P < .01$ from unexposed PBMCs; $^{**}P < .01$ from PBMC + UV-HSV-1. (F-G) Purified NK cells were exposed, or not, to UV-HSV-1 for 60 minutes, and the cellular localization of the NF-κB p65 subunit was determined by fluorescent immunohistochemistry. Bar graph represents manual scoring of translocation from ≥500 cells and 6 different fields. $^*P < .0005$ from unexposed PBMCs. White bar on images indicates 100-μm interval.

UV-HSV-1–treated PBMCs were not cytolytic toward MSCs (data not shown). The above data suggest that MSC coculture may not afford complete protection from HSV-1 (or UV-HSV-1)–stimulated cytolysis.

UV-HSV-1 directly stimulates the cytolytic potential of NK cells against leukemic but not normal allogeneic lymphocytes

A priori we hypothesized that the observed antileukemic effects were mediated by innate immune cells, because none of our healthy donors had ever been vaccinated with leukemia antigens. Indeed, on a per cell basis, purified $CD4^+$ or $CD8^+$ cells pre-exposed to UV-HSV-1 (0.1 pfu/cell; 16 hours) were significantly less effective at inducing cytolysis of OCI-AML3 cells than purified $CD56^+$ cells identically pre-exposed to UV-HSV-1 (Figure 2C). Conversely, as shown in supplemental Figure 2A, depletion of $CD56^+$ cells from PBMCs largely abrogated the increased cytolytic potential observed with their undepleted counterparts after exposure to UV-HSV-1. Moreover, UV-HSV-1 also potentiated cytolytic activity of purified $CD56^+$ cells against the prototypical NK target cell line, K562, in a standard ^{51}Cr release assay (supplemental Figure 2B). These data suggest that NK cells are directly activated by UV-HSV-1 and support our hypothesis that they play a major role in the observed antileukemic effects. In addition, because NK cells are thought to recognize missing-self signals in target cells, we asked whether PBMCs pre-exposed to UV-HSV-1 would induce cytolysis of healthy allogeneic lymphocytes. As shown in Figure 2D-E, PBMCs previously exposed to UV-HSV-1 were incapable of inducing cytolysis of allogeneic lymphocytes, even though they potently induce cytolysis of OCI-AML3 cells. Likewise, no cytolysis of healthy allogeneic monocytes was observed in these assays (data not shown). These data demonstrate that, at least in vitro, UV-HSV-1 stimulation of PBMCs induces selective cytolysis of malignant cells.

UV-HSV-1 rapidly stimulates the cytolytic potential of NK cells via TLR-2/NF-κB signaling

To gain insight into the kinetics of activation of PBMCs exposed to UV-HSV-1, we performed a time-course study with cells from 2 separate donors by exposing them to UV-HSV-1 (0.1 pfu/PBMC)

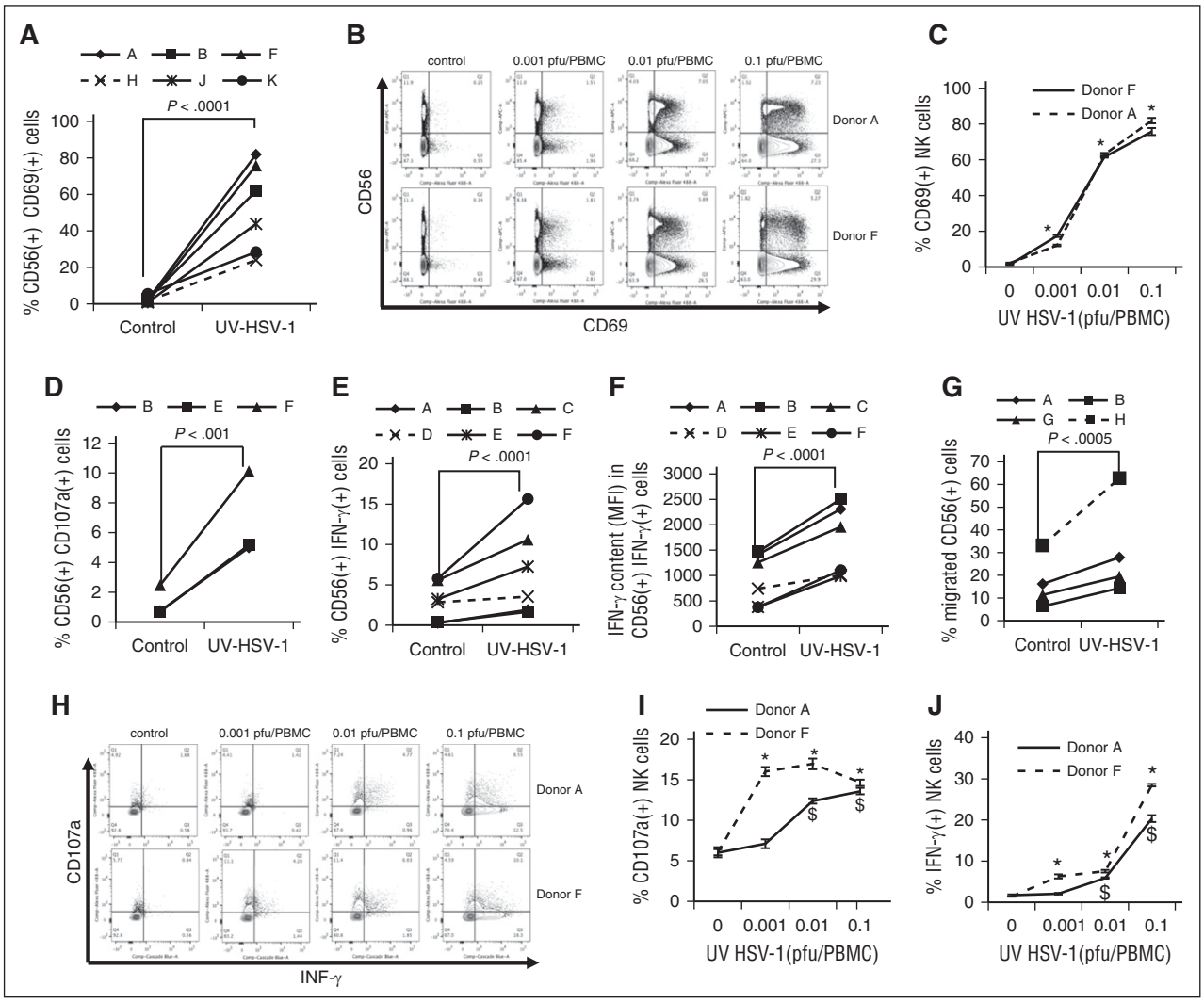

Figure 4. UV-HSV-1 potently induces activation of NK cells. (A) PBMCs from 6 healthy donors were exposed to UV-HSV-1 (0.1 pfu/PBMC for 16 hours), and expression of CD69 was determined by flow cytometry as described in "Materials and methods." (B-C) PBMCs from 2 healthy donors were exposed to increasing concentrations of UV-HSV-1 for 16 hours, and CD69 expression was determined by flow cytometry. $^*P < .001$ from unexposed PBMCs. (D) PBMCs from 3 healthy donors were exposed to UV-HSV-1 (0.1 pfu/PBMC for 16 hours) and degranulation (CD107a externalization) was determined by flow cytometry as described in "Materials and methods." (E-F) PBMCs from 6 healthy donors were exposed to UV-HSV-1 (0.1 pfu/PBMC for 16 hours), and the % of cells positive for IFN-γ and the relative amounts of IFN-γ in positive cells were determined by flow cytometry as described in "Materials and methods." (G) PBMCs from 3 healthy donors were exposed to UV-HSV-1 (0.1 pfu/PBMC for 16 hours), and migration toward OCI-AML3 conditioned media was determined by flow cytometry as described in "Materials and methods." (H-J) PBMCs from 2 healthy donors were exposed to increasing concentrations of UV-HSV-1 for 16 hours, and CD107a externalization and % of IFN-γ^+ cells was determined by flow cytometry. $^*P < .05$ from unexposed controls.

for 1, 4, and 16 hours. As shown in Figure 3A-B, UV-HSV-1 significantly increased the cytolytic potential of PBMCs as early as 1 hour after exposure, particularly in the donor with higher $CD56^+$ content, and this effect was most apparent at higher effector:target cell ratios. Because HSV-1 has been shown to activate TLR-2 signaling in NK cells,[21] we asked whether neutralizing antibodies against TLR-2 (clone TL2.1) would antagonize the increased cytolytic potential of PBMCs or NK cells exposed to UV-HSV-1. As shown in Figure 3C, clone TL2.1 (10 μg/mL) significantly inhibited cytolysis by UV-HSV-1–activated PBMCs or NK cells (0.1 pfu/cell), whereas isotype-matched antibodies against NKG2C or NKG2D did not (data not shown). Similar inhibitory effects were observed with the protein synthesis inhibitor cycloheximide (10 μg/mL), supporting the notion that UV-HSV-1 activates TLR-2–dependent signaling pathways that lead to de novo protein synthesis. As NF-κB is critically involved in mediating gene expression in response to TLR signaling,[25] we then asked whether pharmacologic inhibition of IκB kinase would antagonize the cytolytic effects of UV-HSV-1–activated PBMCs. As shown in Figure 3D, treatment of PBMCs with the highly selective IκB kinase inhibitor, Bay-11-7082 (1 μM), potently inhibited the effects of UV-HSV-1, and similar results were observed using purified $C56^+$ cells (Figure 3E). Moreover, exposure of purified $CD56^+$ cells to UV-HSV-1 (0.1 pfu/PBMC) for 60 minutes resulted in a significant ($P < .0005$) threefold increase in nuclear translocation of NF-κB as evidenced by fluorescent immunohistochemistry against the NF-κB p65 subunit (Figure 3F-G). Exposure of PBMCs to various TLR ligands also increased cytolytic potential (supplemental Figure 3), suggesting that TLR signaling within PBMCs can be modulated to enhance their antitumor potential. Last, Bay-11-7082 also inhibited cytokine production from purified NK cells treated with UV-HSV-1 (supplemental Figure 4). Taken together, these results suggest that UV-HSV-1 activates the cytolytic potential of PBMCs and isolated NK cells, at least in part, via TLR-2/NF-κB signaling.

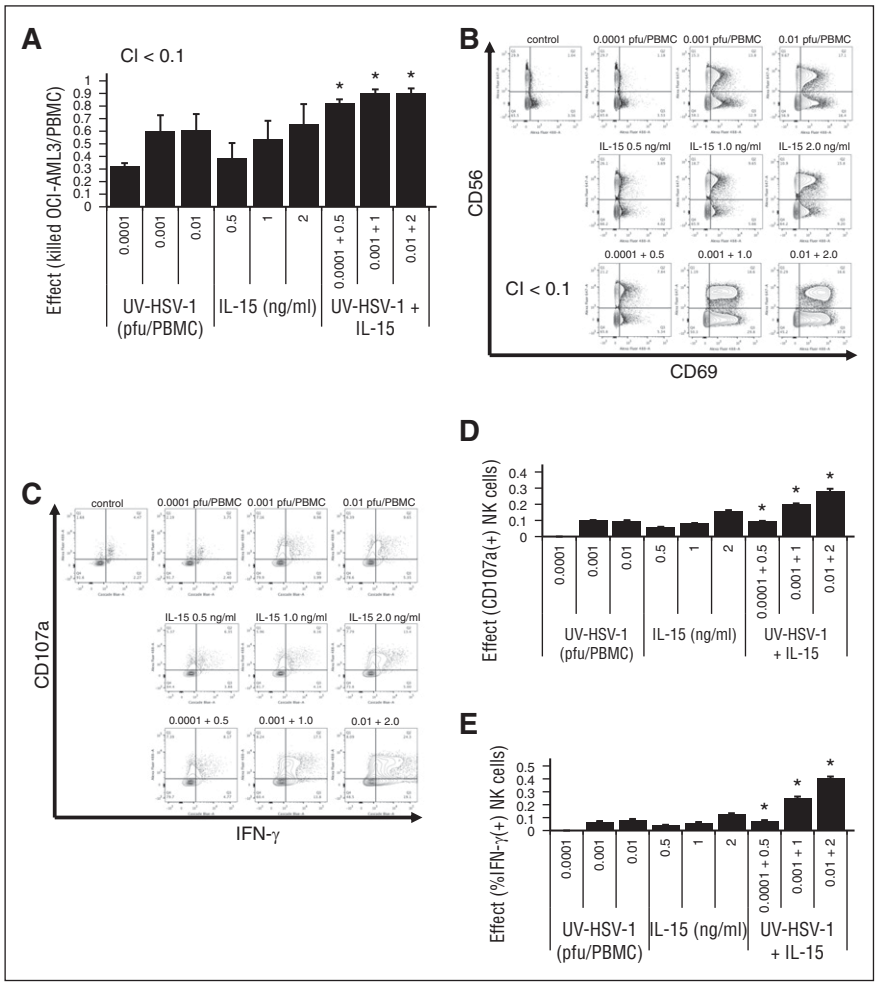

Figure 5. UV-HSV-1 synergizes with IL-15 in activating PBMCs to induce cytolysis of leukemic cells. (A) Isobologram analysis of the interaction of UV-HSV-1 and IL-15 in stimulating PBMC-induced cytolysis of OCI-AML3 (30:1 effector:target). A fixed dose increase (5:1; UV-HSV-1:IL15) was used. *$P < .05$ from UV-HSV-1 or IL-15 alone. (B) Representative flow cytometry plots of an isobologram analysis of the interaction of UV-HSV-1 and IL-15 in stimulating expression of CD69 in NK cells (5:1 fixed dose increase). (C-E) Isobologram analysis of the interaction of UV-HSV-1 and IL-15 in stimulating degranulation and expression of IFN-γ in NK cells (5:1 fixed dose increase). *$P < .01$ from UV-HSV-1 or IL-15 alone.

UV-HSV-1 potently activates NK cells and promotes their degranulation, IFN-γ production, and migration

CD69 is a human transmembrane C-type lectin that is involved in, and serves as a biomarker of, the functional activation and cytolytic potential of NK cells.[26,27] We thus asked if UV-HSV-1 promoted an increase in CD69 expression on the surface of NK cells. As shown in Figure 4A, UV-HSV-1 (0.1 pfu/PBMC) did indeed induce a significant ($P < .0001$) increase in the percent of NK cells expressing CD69, reaching ~80% of total NK cells in some donors. Importantly, although UV-HSV-1 also induced activation on non-NK cells (Figure 4B), the maximal expression of CD69 in this compartment did not surpass ~33%, indicating that NK cells are preferentially activated by this agent. Moreover, UV-HSV-1 elicited significant dose-dependent increases in CD69 expression in NK cells, starting at doses as low as 0.001 pfu/PBMC (Figure 4C), suggesting that HSV-1 antigens are very potent activators of NK cells. To then investigate whether the upregulation of CD69 correlated with degranulation and cytokine production, we monitored CD107a externalization (a marker of degranulation) and intracellular levels of IFN-γ in NK cells after exposing UV-HSV-1–treated PBMCs to OCI-AML3 cells for 6 hours. As shown in Figure 4D, UV-HSV-1 at a dose of 0.1 pfu/PBMC promoted significant degranulation of NK cells, and similar results were observed with purified NK cells exposed to UV-HSV-1 (supplemental Figure 5). In addition, UV-HSV-1 increased the percent of IFN-γ^+ NK cells (Figure 4E), as well as the relative amounts of IFN-γ produced by these cells (Figure 4F). Of note, degranulation and IFN-γ production were significantly inhibited (>50%) by Bay-11-7082, suggesting that TLR-2/NF-κB signaling contributes to these responses (supplemental Figure 16). Furthermore, as shown in Figure 4G, UV-HSV-1 (0.1 pfu/PBMC; 16-hour exposure) significantly ($P < .05$) increased (by approximately twofold) the migration of NK cells toward OCI-AML3–conditioned medium. Last, dose–response studies (Figure 4H-J) confirmed that doses as low as 0.01 pfu/PBMC induced significant ($P < .05$) expression of IFN-γ and degranulation in NK cells from 2 healthy donors. These results strongly argue that UV-HSV-1 is a bona fide activator of NK-cell function.

UV-HSV-1 synergizes with IL-15 in promoting activation and cytolytic potential of NK cells

Because IL-15 is a potent activator of NK effector functions,[28] we asked whether UV-HSV-1 would synergize with IL-15 in promoting PBMC-induced cytolysis of leukemic cells. Isobologram analysis of the combination of UV-HSV-1 with IL-15 (Figure 5A) revealed combination indices of <0.1, suggesting that UV-HSV-1 indeed synergizes with this cytokine to stimulate PBMC-induced killing of leukemic cells in culture. Additionally, as shown in Figure 5B-E, the combination of UV-HSV-1 with IL-15 synergically (combination index <0.1) induced CD69 expression and markedly enhanced the degranulation and IFN-γ production of NK cells. These observations support the notion that UV-HSV-1 and IL-15 promote activation and cytolytic potential of NK cells via complementary mechanisms and thus provide a rationale for possible combinatorial strategies of these 2 agents for improving

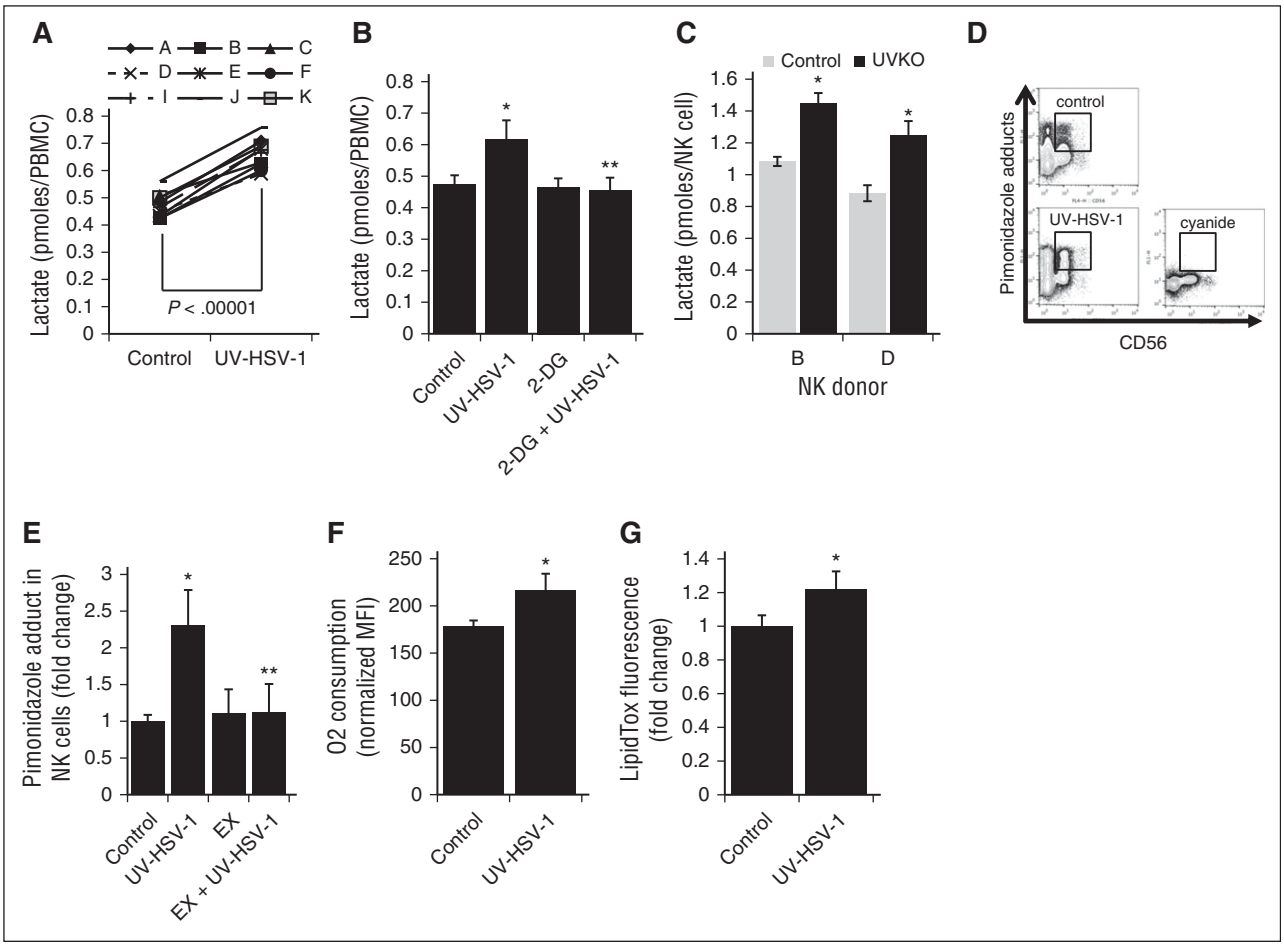

Figure 6. UV-HSV-1 induces metabolic reprogramming of NK cells. (A) PBMCs from 9 healthy donors were exposed to UV-HSV-1 (0.1 pfu/PBMC for 16 hours), and the levels of lactate in the culture supernatant were quantitated as described in "Materials and methods." Results are expressed as pmol lactate/cell. (B) PBMCs from 4 healthy donors were exposed to UV-HSV-1 (0.1 pfu/PBMC for 16 hours), ±11 mM 2-deoxyglucose and lactate levels determined as above. *$P < .01$ from control; **$P < .01$ from UV-HSV-1. (C) NK cells from 2 healthy donors were exposed to UV-HSV-1 (0.1 pfu/PBMC for 16 hours), and the levels of lactate in the culture supernatant were quantitated. *$P < .05$ from control. (D) Representative flow cytometry plots of oxygen consumption measurements using pimonidazole as an indicator of cellular respiration. (E) PBMCs from 4 healthy donors were exposed to UV-HSV-1 (0.1 pfu/PBMC), ±100 μM etomoxir for 4 h in complete medium supplemented with pimonidazole, and the accumulation of pimonidazole adducts was quantitated as described in "Materials and methods." PBMCs treated with 6 mM sodium cyanide served as a background control, and results are shown as cyanide-corrected values. Each donor was tested in triplicate, and the average value was used for statistical purposes. *$P < .05$ from control; **$P < .05$ from UV-HSV-1 alone. (F) EasySep purified $CD56^+$ cells were exposed, or not, to 0.1 pfu/NK cell UV-HSV-1 for 4 hours in complete medium supplemented with pimonidazole, and the accumulation of pimonidazole adducts was quantitated as above. *$P < .05$ from control. (G) PBMCs from 3 healthy donors were exposed to 0.1 pfu/PBMC UV-HSV-1 for 16 hours, and the accumulation of intracellular triglycerides was monitored by flow cytometry as described in "Materials and methods." Each donor was tested in triplicate, and the average value was used for statistical purposes. *$P < .05$ from control.

innate antileukemic responses. Similar observations were made with UV-HSV-1 in combination with IL-2 (supplemental Figure 7).

UV-HSV-1 promotes metabolic reprogramming of NK cells

During the course of our experiments, we noted that UV-HSV-1–treated PBMCs increased the acidity of RPMI-1640 medium (data not shown). We therefore hypothesized that, because immune effector functions tend to be associated with increased glycolysis,[29] UV-HSV-1 might promote an increase in lactate generation in PBMCs. Indeed, as shown in Figure 6A, UV-HSV-1 promoted a significant ($P < .00001$) 40% increase in lactate generation among all donors examined. Moreover, this increase was completely abrogated by the hexokinase inhibitor 2-deoxyglucose (2-DG; Figure 6B), suggesting that UV-HSV-1 activates glycolysis in PBMCs. As well, as shown in Figure 6C, purified NK cells that were exposed after isolation to UV-HSV-1 (0.1 pfu/NK cell; 16 hours) also increased the generation of lactate, suggesting that UV-HSV-1 can directly reprogram NK cells to increase their nonoxidative metabolism of glucose carbon skeletons. To then determine whether UV-HSV-1 modulates mitochondrial function, we monitored oxygen consumption by flow cytometry using the reduction of pimonidazole as a surrogate marker for oxygen consumption as described in "Materials and methods." As shown in Figure 6D-E, UV-HSV-1 promoted a rapid (within 4 hours after exposure) increase in oxygen consumption in NK cells, and this increase was completely abrogated by etomoxir, an inhibitor of fatty acid oxidation (FAO). This increase in oxygen consumption was also observed using a phosphorescent oxygen-sensitive probe in PBMCs treated with UV-HSV-1 (supplemental Figure 8). Of note, as shown in Figure 6F, UV-HSV-1 directly stimulated an increase in oxygen consumption in purified $CD56^+$ cells after isolation. Additionally, as shown in supplemental Figure 9, NK cells derived from PBMCs exposed to UV-HSV-1 for 16 hours continued to display increased oxygen consumption, suggesting that the observed increase in mitochondrial function is maintained at the time when lactate generation was monitored. These somewhat surprising results suggest that UV-HSV-1 promotes a switch from the oxidation of glucose carbon skeletons to the oxidation of fatty acids, perhaps allowing Krebs cycle activity to

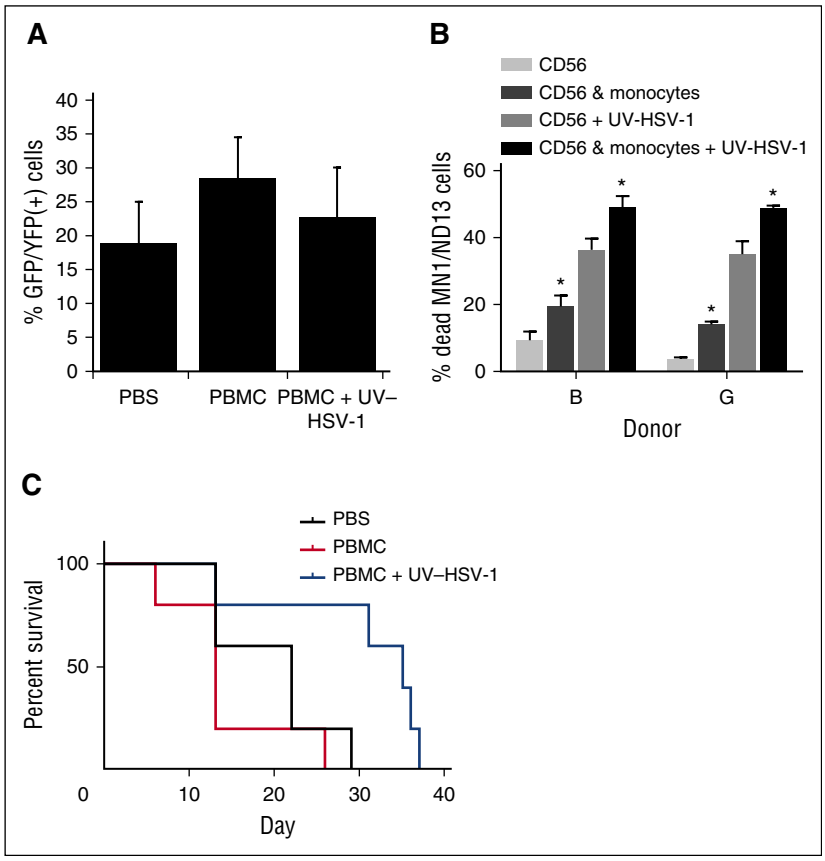

Figure 7. UV-HSV-1 potentiates the therapeutic efficacy of allogeneic donor PBMC infusions in a murine model of human leukemic. (A) Peripheral blood leukemia burden was analyzed by flow cytometry gating on live GFP/YFP$^+$ lymphocytes/monocytes 26 days after implantation of MN1/ND13 cells in sublethally irradiated NRG-3GS mice. (B) Purified NK cells from 2 healthy donors were exposed to 0.1 pfu/PBMC of UV-HSV-1 for 16 hours, ±EasySep-purified autologous monocytes (~85% purity) at a ratio of 2:1 NK: monocyte. After incubation, only floating cells were collected, and their cytolytic activity against MN1/ND13 cells was determined. *$P < .01$ from condition without monocytes. (C) Twenty-eight days after implantation of MN1/ND13 cells, mice were intravenously injected with PBS, T cell–depleted healthy human PBMCs (3×10^6 cells), or T cell–depleted PBMCs exposed ex vivo to UV-HSV-1 (3×10^6 cells; 0.1 pfu/PBMC; 16 hours). Kaplan-Meier analysis was performed on surviving fractions.

proceed while sparing glucose carbon skeletons for biosynthesis. In support of this, UV-HSV-1 (0.1 pfu/PBMC) increased intracellular triglyceride stores in NK cells by ~20% after 16-hour incubation (Figure 6F), suggesting de novo lipid and/or triglyceride biosynthesis. These findings also support the notion of a futile cycle of fatty acid synthesis and FAO in NK cells activated by UV-HSV-1, as has been proposed to occur during the development of memory CD8 cells.[30,31]

Metabolic requirements for cytolysis by UV-HSV-1–activated PBMCs

Because immune effector functions are typically associated with increased glycolysis,[32-34] we then carried out dose–response studies with UV-VSV, UV-Reo, UV-Ad, and UV-HSV-1 and found that UV-HSV-1 was at least ~100-fold more potent in stimulating glycolysis in PBMCs than the other UV-inactivated viruses (supplemental Figure 10A), and, except for UV-AD, increases in lactate generation closely mirrored increases in cytolytic activity (Figure 6G), suggesting the possibility that metabolic reprogramming and cytolytic activity are associated. Similar results were observed with several healthy PBMC donors (data not shown). To then determine how glycolysis and FAO contribute to cytolytic potential, we exposed PBMCs to UV-HSV-1 (0.1 pfu/PBMC) for 16 hours, in the presence or absence of 2-DG or etomoxir, followed by extensive washing and incubation with target cells in the absence of inhibitors. As shown in supplemental Figure 10B, only 2-DG significantly ($P < .005$) inhibited UV-HSV-1–stimulated cytolysis of OCI-AML3 in all 3 donors at a concentration of 11 mM (inhibition ~45% ± 10%); in contrast, etomoxir at the highest dose tested (100 μM) only moderately inhibited killing in 1 of 3 donors tested. Of note, 2-DG at a concentration of 22 mM achieved a more robust ~65% inhibition in 2 donors tested (supplemental Figure 10C), further demonstrating that dose-dependent competitive inhibition of glycolysis can antagonize UV-HSV-1–induced activation of cytolytic activity in PBMCs. Interestingly, treatment with Bay-11-7082 (1 μM) did not antagonize the lactate increase in PBMCs treated with UV-HSV-1 (0.1 pfu/PBMC) for 16 hours (Figure 7D), suggesting that NF-κB does not play a critical role in the observed metabolic reprogramming. On the other hand, treatment with the PKCα/β inhibitor, Go6976 (1 μM), completely abrogated lactate generation (supplemental Figure 10D), suggesting that, as reported for human dendritic cells,[35] PKC may be activated upstream of NF-κB in response to TLR-2 stimulation. Importantly, Go6976 also inhibited cytolysis of OCI-AML3 cells by UV-HSV-1–treated PBMCs or NK cells (supplemental Figure 10E). Together, the above results suggest that UV-HSV-1 promotes PKC-dependent metabolic reprogramming of PBMCs and that this reprogramming mediates, at least in part, their increased antileukemic efficacy.

T cell–depleted UV-HSV-1–activated PBMCs exert a therapeutic benefit in a murine xenograft model of human leukemia

To determine the therapeutic efficacy of UV-HSV-1 in the context of leukemia, we implanted 15 NRG-3GS mice with 5×10^5 MN1/ND13 human leukemic cells as previously described.[22] Four weeks after implantation of MN1/ND13 cells, engraftment was verified by flow cytometry (Figure 7A), and mice were i.v. injected with PBS, T cell–depleted healthy human PBMCs (3×10^6 cells), or T cell–depleted PBMCs exposed ex vivo to UV-HSV-1 (3×10^6 cells; 0.1 pfu/PBMC; 16 hours). We chose T cell–depleted PBMCs rather than purified NK cells because, as shown in Figure 7B, the presence of adherent monocytes significantly ($P < .05$) enhanced both baseline and UV-HSV-1–stimulated NK cytolysis of MN1/ND13 cells. Because monocytes do

not induce marked cytolysis of leukemic cells in culture, alone or after treatment with UV-HSV-1 (data not shown), our observations suggest that these cells serve to potentiate the NK response to the viral vector, presumably via secreted paracrine acting cytokines/chemokines (supplemental Figure 11). Importantly, as shown in Figure 7C, survival was significantly extended in the mice that received UV-HSV-1–conditioned, T cell–depleted PBMCs ($P < .03$ from PBS; $P < .01$ from PBMCs only), supporting the hypothesis that UV-HSV-1 may be a potentially safe and effective adjuvant to T cell–depleted, allogeneic donor mononuclear cell infusions for the treatment of AML.

Discussion

Oncolytic virotherapy has recently demonstrated some success in the treatment of hematologic malignancies, and current thinking is that this is mediated primarily by direct killing of malignant cells and, to a lesser degree, by activation of antileukemic immunity.[15,36,37] Herein we show that HSV-1, both live and UV light–inactivated, activates NK cells to kill leukemic cell lines and primary AML samples. We also show for the first time that UV-HSV-1 is 100- to 1000-fold more potent than UV-inactivated VSV (*Rhabdoviridae*), Reovirus (*Reoviridae*), or Adenovirus (*Adenoviridae*) in promoting PBMC-induced cytolysis of leukemia targets. Two major strains of HSV-1 (1716 and F) demonstrated similar potency, highlighting the potent innate immunogenicity of the *Herpesviridae* family. Related to this, intriguing clinical evidence over the past 3 decades has suggested that, at least in the context of BMT for the therapy of AML, reactivation of CMV, a β-subfamily member of *Herpesviridae*, reduces the risk of leukemia relapse and improves survival.[19,20,38] Because CMV is not oncolytic per se and because it has been shown to promote the generation of memory-like NK cells in humans and mice,[17,18] it is conceivable that activation of innate immunity in response to CMV may be critical for the control of leukemia progression and relapse. Furthermore, another member of the *Herpesviridae* family, Herpes simplex virus (α subfamily), has recently been reported to directly stimulate NK cells to produce IFN-γ, increase CD69 and major histocompatibility complex class II expression, and facilitate antigen presentation to $CD4^+$ T cells.[21] Given the promising therapeutic benefit that allogeneic NK cell infusions offer myeloid leukemia patients in the absence of widespread graft-versus-host disease,[3,39-41] it is tempting to speculate that members of the α *Herpesviridae* family may further improve the anti-leukemic efficacy of "off-the-shelf" (eg, expanded from umbilical cord blood or other allogeneic source) NK cells. Indeed, our in vivo experiment demonstrated for the first time a significant survival advantage of leukemic mice treated with T cell–depleted PBMCs previously exposed to UV-HSV-1, suggesting that UV-HSV-1 may be a potentially safe and effective adjuvant for allogeneic donor mononuclear cell infusions (after BMT) or haploidentical NK cell infusions for the treatment of leukemia.

The antileukemic effects of NK cells treated with UV-HSV-1 appear to be NF-κB dependent, and various TLR agonists partially recapitulate this effect, supporting previous work from Kim et al demonstrating that antigens from both HSV-1 and HSV-2 can directly activate NK cells via TLR signaling.[21] Mechanistically, we found that UV-HSV-1 promotes dose-dependent expression of CD69, production of IFN-γ, degranulation, and migration of NK cells, demonstrating a profound effect on innate immune function and phenotype. Moreover, the striking potency of UV-HSV-1 supports a "kiss and run model," whereby a single viral particle may be able to activate several NK cells. Importantly, we show that UV-HSV-1 synergizes with IL-15 in promoting NK-cell activation and antileukemic efficacy, suggesting that complimentary pathways can be modulated to further enhance the therapeutic potential of NK cells.

We also demonstrate for the first time that activation of NK cells by UV-HSV-1 is associated with both increased generation of lactate and increased FAO-dependent oxygen consumption. Curiously, however, only glycolysis appears to be critical for their enhanced antileukemic effects. These observations are partly in agreement with previous work demonstrating that immune effector functions are associated with a glycolytic phenotype.[32-34] Nonetheless, our observation that UV-HSV-1 increases FAO-dependent oxygen consumption is somewhat surprising because FAO is a biochemical pathway more often associated with the function of memory CD8 T cells.[42] Moreover, the pharmacologic FAO inhibitor, etomoxir, at doses sufficient to repress oxygen consumption in UV-HSV-1–stimulated NK cells, did not significantly antagonize NK-induced cytolysis of leukemic cells in several donors. This suggests that fatty acid metabolism does not support this particular effector function. Paradoxically, although we demonstrate that FAO supports the molecular reduction of oxygen in NK cells, we also provide evidence that UV-HSV-1 induces de novo fatty acid synthesis in NK cells. These particular findings resonate with a recent report by O'Sullivan et al demonstrating that CD8 memory T cells use glucose-derived carbon skeletons for the synthesis of fatty acids, which are then oxidized in the mitochondria via FAO.[30] The significance of this "futile cycle" remains to be fully understood, but it highlights a metabolic plasticity in the immune system that may be required to promote survival of memory cells. Given the high prevalence (~50%) of HSV-1 seropositivity in North America,[43,44] it is enticing to suggest that perhaps HSV-1 exposure induces memory-like NK cells, as observed for CMV, that rapidly respond to UV-HSV-1 by modulating their fatty acid metabolism. Alternatively, given that 100% of the donors tested in this study responded rapidly to UV-HSV-1, it is also plausible that this vector induces metabolic reprogramming independent of prior exposure.

In conclusion, our findings demonstrate for the first time that *Herpesviridae* family members are potent stimulators of innate immune function, and that these vectors could in principle be used for therapeutic purposes in the treatment of leukemia. Future studies should investigate whether synthetic TLR agonists (alone or in combinations) could substitute for UV-HSV-1, as well as focus on possible combinatorial strategies with IL-15 or IL-2 to further enhance the therapeutic efficacy of allogeneic donor mononuclear cell or NK infusions.

Acknowledgments

The authors thank Shera Patterson and Christine Kelly for administrative assistance, Karen Lambie for technical assistance, and the BC Cancer Agency Hematology Cell Bank for providing frozen primary leukemia samples and MSCs.

This work was funded by grants from Departamento Administrativo de Ciencia, Tecnología e Innovación (projects 120351929072 and 210157636410) (I.S.); the Lotte & John Hecht Memorial Foundation, with core support from the British Columbia Cancer Foundation and the British Columbia Cancer Agency (G.K.); and the Terry Fox Foundation of Canada (K.H.).

Authorship

Contribution: I.S. designed research, performed research, analyzed data, and wrote the paper; S.I. designed research and contributed vital reagents; H.S., E.H., M.N., J.T.C.L., V.L., and M.G. performed

research; G.F.T.P. and F.T. designed research; L.B. and G.L. contributed vital reagents; and K.R., K.H., W.J., and G.K. designed research, analyzed data, and wrote the paper.

Conflict-of-interest disclosure: W.J. is a shareholder and director of ViroGin Biotech Ltd, which develops oncolytic viruses for cancer treatment. All other authors declare no competing financial interests.

Correspondence: Gerald Krystal, Terry Fox Laboratory, British Columbia Cancer Agency, Vancouver, BC V5Z 1L3, Canada; e-mail: gkrystal@bccrc.ca.

References

1. Estey EH. Acute myeloid leukemia: 2013 update on risk-stratification and management. *Am J Hematol.* 2013;88(4):318-327.
2. Magenau J, Tobai H, Pawarode A, et al. Clofarabine and busulfan conditioning facilitates engraftment and provides significant antitumor activity in nonremission hematologic malignancies. *Blood.* 2011;118(15): 4258-4264.
3. Bachanova V, Cooley S, Defor TE, et al. Clearance of acute myeloid leukemia by haploidentical natural killer cells is improved using IL-2 diphtheria toxin fusion protein. *Blood.* 2014;123(25):3855-3863.
4. Miller JS, Soignier Y, Panoskaltsis-Mortari A, et al. Successful adoptive transfer and in vivo expansion of human haploidentical NK cells in patients with cancer. *Blood.* 2005;105(8): 3051-3057.
5. Davies JO, Stringaris K, Barrett AJ, Rezvani K. Opportunities and limitations of natural killer cells as adoptive therapy for malignant disease. *Cytotherapy.* 2014;16(11):1453-1466.
6. Shen Y, Nemunaitis J. Herpes simplex virus 1 (HSV-1) for cancer treatment. *Cancer Gene Ther.* 2006;13(11):975-992.
7. Kim JH, Oh JY, Park BH, et al. Systemic armed oncolytic and immunologic therapy for cancer with JX-594, a targeted poxvirus expressing GM-CSF. *Molec Therap.* 2006;14(3):361-370.
8. Kirn DH, Wang Y, Le Boeuf F, Bell J, Thorne SH. Targeting of interferon-beta to produce a specific, multi-mechanistic oncolytic vaccinia virus. *PLoS Med.* 2007;4(12):e353.
9. Liu TC, Hwang TH, Bell JC, Kirn DH. Translation of targeted oncolytic virotherapeutics from the lab into the clinic, and back again: a high-value iterative loop. *Mol Ther.* 2008;16(6):1006-1008.
10. Lorence RM, Roberts MS, O'Neil JD, et al. Phase 1 clinical experience using intravenous administration of PV701, an oncolytic Newcastle disease virus. *Curr Cancer Drug Targets.* 2007; 7(2):157-167.
11. Msaouel P, Dispenzieri A, Galanis E. Clinical testing of engineered oncolytic measles virus strains in the treatment of cancer: an overview. *Curr Opin Mol Ther.* 2009;11(1):43-53.
12. Smith KD, Shao MY, Posner MC, Weichselbaum RR. Tumor genotype determines susceptibility to oncolytic herpes simplex virus mutants: strategies for clinical application. *Future Oncol.* 2007;3(5): 545-556.
13. Yu W, Fang H. Clinical trials with oncolytic adenovirus in China. *Curr Cancer Drug Targets.* 2007;7(2):141-148.
14. Liu TC, Galanis E, Kirn D. Clinical trial results with oncolytic virotherapy: a century of promise, a decade of progress. *Nat Clin Pract Oncol.* 2007; 4(2):101-117.
15. Russell SJ, Federspiel MJ, Peng KW, et al. Remission of disseminated cancer after systemic oncolytic virotherapy. *Proc Mayo Clinic.* 2014; 89(7):926-933.
16. Chan CJ, Smyth MJ, Martinet L. Molecular mechanisms of natural killer cell activation in response to cellular stress. *Cell Death Differ.* 2014;21(1):5-14.
17. Foley B, Cooley S, Verneris MR, et al. Human cytomegalovirus (CMV)-induced memory-like NKG2C(+) NK cells are transplantable and expand in vivo in response to recipient CMV antigen. *J Immunol.* 2012;189(10):5082-5088.
18. Arase H, Mocarski ES, Campbell AE, Hill AB, Lanier LL. Direct recognition of cytomegalovirus by activating and inhibitory NK cell receptors. *Science.* 2002;296(5571):1323-1326.
19. Green ML, Leisenring WM, Xie H, et al. CMV reactivation after allogeneic HCT and relapse risk: evidence for early protection in acute myeloid leukemia. *Blood.* 2013;122(7):1316-1324.
20. Lönnqvist B, Ringdèn O, Ljungman P, Wahren B, Gahrton G. Reduced risk of recurrent leukaemia in bone marrow transplant recipients after cytomegalovirus infection. *Br J Haematol.* 1986; 63(4):671-679.
21. Kim M, Osborne NR, Zeng W, et al. Herpes simplex virus antigens directly activate NK cells via TLR2, thus facilitating their presentation to CD4 T lymphocytes. *J Immunol.* 2012;188(9): 4158-4170.
22. Imren S, Heuser M, Gasparetto M, et al. Modeling de novo leukemogenesis from human cord blood with MN1 and NUP98HOXD13. *Blood.* 2014; 124(24):3608-3612.
23. Samudio I, Harmancey R, Fiegl M, et al. Pharmacologic inhibition of fatty acid oxidation sensitizes human leukemia cells to apoptosis induction. *J Clin Invest.* 2010;120(1):142-156.
24. Miller PH, Cheung AM, Beer PA, et al. Enhanced normal short-term human myelopoiesis in mice engineered to express human-specific myeloid growth factors. *Blood.* 2013;121(5):e1-e4.
25. Ozato K, Tsujimura H, Tamura T. Toll-like receptor signaling and regulation of cytokine gene expression in the immune system. *Biotechniques.* 2002;33(4 Suppl):S65-S75.
26. Clausen J, Vergeiner B, Enk M, Petzer AL, Gastl G, Gunsilius E. Functional significance of the activation-associated receptors CD25 and CD69 on human NK-cells and NK-like T-cells. *Immunobiology.* 2003;207(2):85-93.
27. Dons'koi BV, Chernyshov VP, Osypchuk DV. Measurement of NK activity in whole blood by the CD69 up-regulation after co-incubation with K562, comparison with NK cytotoxicity assays and CD107a degranulation assay. *J Immunol Methods.* 2011;372(1-2):187-195.
28. Alnabhan R, Madrigal A, Saudemont A. Differential activation of cord blood and peripheral blood natural killer cells by cytokines. *Cytotherapy.* 2014;17(1):73-85.
29. Pearce EL, Poffenberger MC, Chang CH, Jones RG. Fueling immunity: insights into metabolism and lymphocyte function. *Science.* 2013; 342(6155):1242454.
30. O'Sullivan D, van der Windt GJ, Huang SC, et al. Memory CD8(+) T cells use cell-intrinsic lipolysis to support the metabolic programming necessary for development. *Immunity.* 2014;41(1):75-88.
31. Weinberg SE, Chandel NS. Futility sustains memory T cells. *Immunity.* 2014;41(1):1-3.
32. Gubser PM, Bantug GR, Razik L, et al. Rapid effector function of memory CD8+ T cells requires an immediate-early glycolytic switch. *Nat Immunol.* 2013;14(10):1064-1072.
33. van der Windt GJ, O'Sullivan D, Everts B, et al. CD8 memory T cells have a bioenergetic advantage that underlies their rapid recall ability. *Proc Natl Acad Sci USA.* 2013;110(35): 14336-14341.
34. Donnelly RP, Loftus RM, Keating SE, et al. mTORC1-dependent metabolic reprogramming is a prerequisite for NK cell effector function. *J Immunol.* 2014;193(9):4477-4484.
35. Langlet C, Springael C, Johnson J, et al. PKC-alpha controls MYD88-dependent TLR/IL-1R signaling and cytokine production in mouse and human dendritic cells. *Eur J Immunol.* 2010;40(2): 505-515.
36. Castleton A, Dey A, Beaton B, et al. Human mesenchymal stromal cells deliver systemic oncolytic measles virus to treat acute lymphoblastic leukemia in the presence of humoral immunity. *Blood.* 2014;123(9): 1327-1335.
37. Batenchuk C, Le Boeuf F, Stubbert L, et al. Non-replicating rhabdovirus-derived particles (NRRPs) eradicate acute leukemia by direct cytolysis and induction of antitumor immunity. *Blood Cancer J.* 2013;3:e123.
38. Elmaagacli AH, Steckel NK, Koldehoff M, et al. Early human cytomegalovirus replication after transplantation is associated with a decreased relapse risk: evidence for a putative virus-versus-leukemia effect in acute myeloid leukemia patients. *Blood.* 2011;118(5):1402-1412.
39. Linn YC, Niam M, Chu S, et al. The anti-tumour activity of allogeneic cytokine-induced killer cells in patients who relapse after allogeneic transplant for haematological malignancies. *Bone Marrow Transplant.* 2012;47(7):957-966.
40. Linn YC, Yong HX, Niam M, et al. A phase I/II clinical trial of autologous cytokine-induced killer cells as adjuvant immunotherapy for acute and chronic myeloid leukemia in clinical remission. *Cytotherapy.* 2012;14(7):851-859.
41. Norell H, Moretta A, Silva-Santos B, Moretta L. At the Bench: preclinical rationale for exploiting NK cells and γδ T lymphocytes for the treatment of high-risk leukemias. *J Leukoc Biol.* 2013;94(6): 1123-1139.
42. Pearce EL, Walsh MC, Cejas PJ, et al. Enhancing CD8 T-cell memory by modulating fatty acid metabolism. *Nature.* 2009;460(7251):103-107.
43. Gorfinkel IS, Aoki F, McNeil S, et al. Seroprevalence of HSV-1 and HSV-2 antibodies in Canadian women screened for enrolment in a herpes simplex virus vaccine trial. *Int J STD AIDS.* 2013;24(5):345-349.
44. Bradley H, Markowitz LE, Gibson T, McQuillan GM. Seroprevalence of herpes simplex virus types 1 and 2–United States, 1999-2010. *J Infect Dis.* 2014;209(3):325-333.